



Carbon-dot-based ratiometric fluorescence glucose biosensor

Moon-Jin Cho, Soo-Young Park*

Department of Polymer Science & Engineering, Polymeric Nanomaterials Laboratory, School of Applied Chemical Engineering, Kyungpook National University, 80 Daehak-ro, Buk-gu, Daegu 41566, Republic of Korea

ARTICLE INFO

Keywords:

Carbon dot
Biosensor
Ratiometric
Fluorescence
Glucose
Enzyme

ABSTRACT

A ratiometric fluorescence glucose biosensor based on carbon dots (CDs) and rhodamine 6G (Rh6G) was developed both as an aqueous solution and as a crosslinked poly(acrylic acid) solid-state film. A ratiometric fluorescence color change was realized by fluorescence quenching due to the bienzymatic reaction of glucose oxidase (GOx) and horseradish peroxidase (HRP) with glucose. When excited at 360 nm, the blue fluorescence emission of the CDs, prepared by a solvothermal method with citric acid and ethylene diamine, was quenched by the bienzymatic reaction with glucose, whereas the fluorescence of Rh6G was inert to glucose. Thus, a ratiometric fluorescence color change from blue to green was observed as the glucose concentration increased. The optimized CD/Rh6G/GOx/HRP aqueous solution showed a linear range of 0.1–500 μM with a limit of detection (LOD) of 0.04 μM , good selectivity for glucose over the major ingredients in human blood and could be used with human blood serum. A stable solid-state biosensor film was fabricated by immobilization of CD/Rh6G/GOx/HRP in the hydrogel film prepared by ultraviolet curing of a mixture of acrylic acid and diacrylated poly(ethylene glycol) (70:30, w/w). Compared to the CD/Rh6G/GOx/HRP aqueous solution, the hydrogel film showed a similar ratiometric fluorescence color change, sensitivity (linear range of 0.5–500 μM with an LOD of 0.08 μM), and selectivity. Further, the solid-state glucose biosensor film was inherently stable and could be used whenever needed, overcoming the instability of the aqueous solution (owing to aggregation, enzyme denaturation, etc.). These ratiometric biosensors increase the ability to detect glucose using the naked eye compared to simple turn-on or turn-off modes. Thus, this approach expands the potential applications of CDs in biosensors to provide more convenient and practical detection methods.

1. Introduction

Glucose levels in the human body are one of the most important indicators of a healthy life. In particular, diabetes patients need to test their glucose levels daily [1]. Thus, there is a high demand for accurate, continuous, and noninvasive sensing methods to measure glucose levels to simplify the testing process and improve its specificity. Biosensors have three main parts, namely a biological recognition element, a transducer, and a signal processing system [2–4]. Typical molecular recognition elements include receptors, enzymes, antibodies, nucleic acids, microorganisms, and lectins [5,6]. The principal methods used in the transducer are electrochemical, optical, thermometric, piezoelectric, and magnetic [7]. Transducers in current glucose biosensors are mainly electrochemical due to better sensitivity, reproducibility,

easy maintenance, and low cost. Electrochemical sensors may be subdivided into potentiometric, amperometric, or conductometric types [8–10]. The most common commercially available devices are enzymatic amperometric glucose biosensors, which have been widely studied over the last few decades; however, only few non-enzymatic electrochemical glucose sensors have been reported [11–16]. Enzymatic amperometric glucose biosensors monitor currents generated by enzymatic reactions [17,18]. The typical enzyme system used in glucose measurements is the bienzymatic reaction of glucose oxidase (GOx) and horseradish peroxidase (HRP) [19,20]. GOx decomposes glucose into gluconic acid and H_2O_2 , and HRP transforms the produced H_2O_2 into electrons and OH radicals (Scheme 1). This system has relatively high selectivity for glucose, is easy to obtain, cheap, and can withstand extremes of pH, ionic strength, and temperature, thus

Abbreviations: CD, carbon dot; A-CD, acryl groups-functionalized CD; Rh6G, rhodamine 6G; GOx, glucose oxidase; HRP, horseradish peroxidase; PAA, poly(acrylic acid); DAPEG, diacrylated poly(ethylene glycol); TPS, trichloro(1H,1H,2H,2H-perfluorooctyl)silane; CA, citric acid; EDA, ethylene diamine; GMA, glycidyl methyl methacrylate; EDC, 1-(3-(Dimethylaminopropyl)-3-ethylcarbodiimide hydrochloride); NHS, N-hydroxysuccinimide; Chol, cholesterol; AA, L-ascorbic acid; $C_{\text{CD}}/C_{\text{Rh6G}}$, concentrations of CD, Rh6G; Q_6 , $((F_0 - F)/F_0)$ (degree of quenching)

* Corresponding author.

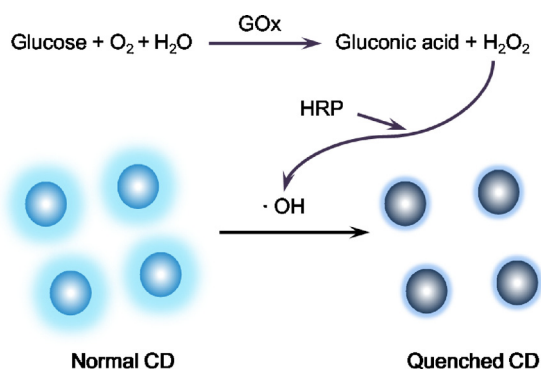
E-mail address: psy@knu.ac.kr (S.-Y. Park).

<https://doi.org/10.1016/j.snb.2018.11.055>

Received 4 July 2018; Received in revised form 25 October 2018; Accepted 11 November 2018

Available online 12 November 2018

0925-4005/ © 2018 Elsevier B.V. All rights reserved.



Scheme 1. Mechanism of CD Quenching by the GOx/HRP bienzyme System.

allowing a wide variety of conditions to be used during the manufacturing process [21,22]. Although there are significant benefits associated with the use of such amperometric glucose biosensors, several difficulties remain, particularly regarding impaired responses, unpredictable drift in the signal in vivo that necessitates frequent calibration against finger-prick samples, complex equipment, sample pre-treatment, etc [23]. Thus, new approaches to glucose sensing in diabetes are being actively explored. Amongst these, fluorescence-based systems are receiving increasing attention [24], encouraged by distinct advantages such as high sensitivity, little or no damage to the host system, the abilities to use time-resolved fluorescence and to probe the structure and distribution of biomolecules by various phenomena, including fluorescence resonance energy transfer (FRET) and photo-induced electron transfer [25]. Fluorescence materials such as quantum dots (QDs) and carbon dots (CDs) have been used as fluorophore probes for glucose detection. Typically, the turn-off mode resulting from fluorescence quenching has been used. For example, H₂O₂ produced by the enzymatic reaction of GOx with glucose can cause the fluorescence quenching of QDs, with the degree of quenching representing the amount of glucose [26]. The turn-on mode based on the photoinduced electron-transfer properties of CDs has also been utilized for glucose sensing [27]. These turn-on and turn-off modes usually use monochromatic fluorescence. However, the fading of color (or the appearance/intensification of color) is sometimes difficult to distinguish with the naked eye.

To increase the visibility of biosensors, two fluorescence fluorophores can be used to induce fluorescence color changes during glucose detection instead of monochromatic turn-on and turn-off modes. The use of fluorescence color changes for analyte detection systems has many advantages because the presence of the analyte can be easily determined using the naked eye. In such systems, the intensity of one fluorescence chromophore is inert to the analyte, whereas that of the other is sensitive to the analyte, so that a ratiometric color change occurs depending on the amount of analyte. For example, fluorescence-quenchable QDs have been used for formaldehyde detection by ratiometric fluorescence color control with the inert fluorescence dye fluorescein [28]. In addition, two different-colored QDs were used for aspirin detection in human saliva, in which red-emitting QDs embedded in SiO₂ nanoparticles acted as the reference signal and green-emitting QDs covalently anchored on the surface of the SiO₂ nanoparticles served as the response signal [29]. Xie et al. reported a dual-emission ratiometric probe based on the red emission of CdTe QDs grafted on the surface of silica particles with the reference dye fluorescein isothiocyanate encapsulated in the particles for glucose detection via bienzyme catalysis (GOx and HRP) [26]. Owing to their excellent optical properties, QDs have attracted wide attention and have been intensively studied in biological applications. However, QDs require further modification for use in biological applications as they are toxic, pose environmental hazards, are susceptible to ultraviolet light excitation, can be photobleached, and are chemically unstable [30]. CDs

are an alternative to QDs for biosensor applications due to their low toxicity and biocompatibility. Boronic-acid-functionalized CDs have been utilized for glucose detection by fluorescence quenching. Fe(III) as a fluorescence quencher has also been used for glucose detection with GOx by a Fenton reaction [31]. In addition, CDs prepared from polyethylene glycol have been used for glucose detection with GOx. The produced H₂O₂ increased the photoluminescence (PL) intensity of the CDs, possibly through oxidation by active oxygen species generated by H₂O₂. However, there have been no reports on glucose detection using ratiometric fluorescence probes based on CDs.

Most glucose sensing platforms with CDs are based on solution biosensors. Aqueous CD solutions are not stable over long periods and enzymes are denatured in water when kept for long times. Thus, solution-based systems are less convenient for use in detection systems as compared to solid systems, such as CD-immobilized films, because dried films are portable and considerably stable over a long period of time. However, reactive groups are required for CD immobilization. Reactive CDs can be realized by introducing reactive groups (e.g., acrylic groups) during bottom-up synthesis. Reactive CDs with urethane acrylate groups have been prepared as fillers in a polymer matrix [32]. CD loading affected the mechanical properties of polyurethane, but the fluorescence properties of the CDs were preserved with good photostability in the polymer matrix. Glycidyl methacrylate (GMA)-functionalized CDs have also been synthesized to produce polymerizable CDs. These CDs have been copolymerized with acrylamide- and methacrylate-type monomers to fabricate transparent hydrogels and 3D solid macrostructures with unique optical properties and excellent biocompatibility [33,34]. However, there have been no reports on color changes in the ratiometric fluorescence emission of CDs in solid-state films.

In this work, CDs prepared from citric acid (CA) and ethylene diamine (EDA) were used for ratiometric fluorescence emission with rhodamine 6 G (Rh6G) in water as a glucose biosensor. The bienzyme system of GOx and HRP induced a ratiometric color change in the CD/Rh6G aqueous solution upon addition of glucose. This CD/Rh6G/GOx/HRP aqueous biosensor solution showed a distinct fluorescence color change with glucose and good sensor performance. The CD/Rh6G/GOx/HRP system was also immobilized in a solid-state hydrogel biosensor film consisting of a poly(acrylic acid) (PAA) film crosslinked with diacrylated poly(ethylene glycol) (DAPEG). This biosensor film also exhibited a fluorescence color change in response to glucose and showed good sensor performance. Thus, the GOx/HRP bienzyme system with ratiometric fluorophores of CD and Rh6G can be applied to biosensor applications in aqueous and solid states, which enable wide application of CDs to biosensors for more convenient and practical detection methods.

2. Experimental

2.1. Materials

DAPEG (weight average molecular weight (M_w) = 400 g/mol) was purchased from Polysciences, USA. Acrylic acid (AA, Junsei, Japan) was used as received. Citric acid (CA, 99.5%), horseradish peroxidase (HRP), *N*-hydroxysuccinimide (NHS), Rh6G, 2-hydroxy-2-methylpropiophenone, trichloro(1*H*,1*H*,2*H*,2*H*-perfluorooctyl)silane (TPS), glycidyl methyl methacrylate (GMA), D-(+)-glucose, urea, uric acid, L-ascorbic acid, lactose, human serum, and benzoylated (MWCO = 2000 Da) membranes were purchased from Sigma-Aldrich, USA. Metal salts of NaCl and CaCl₂, and EDA (99.5%) were obtained from Duksan, South Korea. 1-(3-Dimethylaminopropyl)-3-ethylcarbodiimide hydrochloride (EDC·HCl) was purchased from Tokyo Chemical Industry (TCI), Japan. Deionized (DI) water was used in all experiments after purification through a reverse osmosis system (PureRO, Romax, South Korea).

2.2. Measurements

The UV-vis, PL, and Fourier-transform infrared (FT-IR) spectra were recorded on a UV-2401 PC spectrophotometer (Shimadzu, Japan), an RF-5301 PC (Shimadzu, Japan), and a Jasco FT/IR-620 spectrometer (ATR method, Jasco, Japan), respectively. Photographs of the CD aqueous solutions and DAPEG/AA/CD films were taken with a smartphone camera (SM-G950S, Samsung, South Korea). The sample holder for the solid films during PL measurements aligned the normal of the film 45° to the incident beam and parallel to the ground (Scheme S1). The PL spectra of the aqueous solutions were recorded at pH 7.4 with excitation at 360 nm unless otherwise mentioned. Fluorescence measurements of all the solid-state samples were conducted in a dry state with the same excitation wavelength as for the solution-state samples. Dried films were tested after glucose aqueous solutions directly added to the surface of the film.

2.3. Preparation of CDs and A-CDs

CDs were synthesized according to a previously reported method with a slight modification by using a mini bench-top reactor (Parr series 4560, Parr Instrument Co., USA), as shown in Scheme 2. [35]. Briefly, CA (0.4 g, 0.002 M) and EDA (270 μ L, 0.004 M) were dissolved in DI water (80 mL). When the solution was homogeneous, the mixture was transferred to a bench-top reactor and heated at 160 °C for 5 h. After the reaction, the reactor was cooled to room temperature (24 °C) in air. The produced CD solution, which was brown-red and transparent, was dialyzed in water using a dialysis tube (MWCO = 2000 Da) to obtain pure CDs. To obtain acrylic-group-functionalized CDs (A-CDs), GMA was reacted with the functional groups on the surface of the CDs (Scheme 2). First, 5 mL of CD aqueous solution (5.8 mg/mL) and 0.3 mL of GMA were stirred at 30 °C for 6 h. After the reaction, the oil and water phases were phase-separated. The oil phase was removed and the water phase was washed several times with hexane to remove the small amount of unreacted GMA molecules. Detailed fluorescence results for the CDs can be found in our previous report [36]. The acrylic groups were introduced in the CDs for chemical immobilization owing to covalent bond formation. The chemically immobilized CDs to the DAPEG/AA film are more stable than those without immobilization.

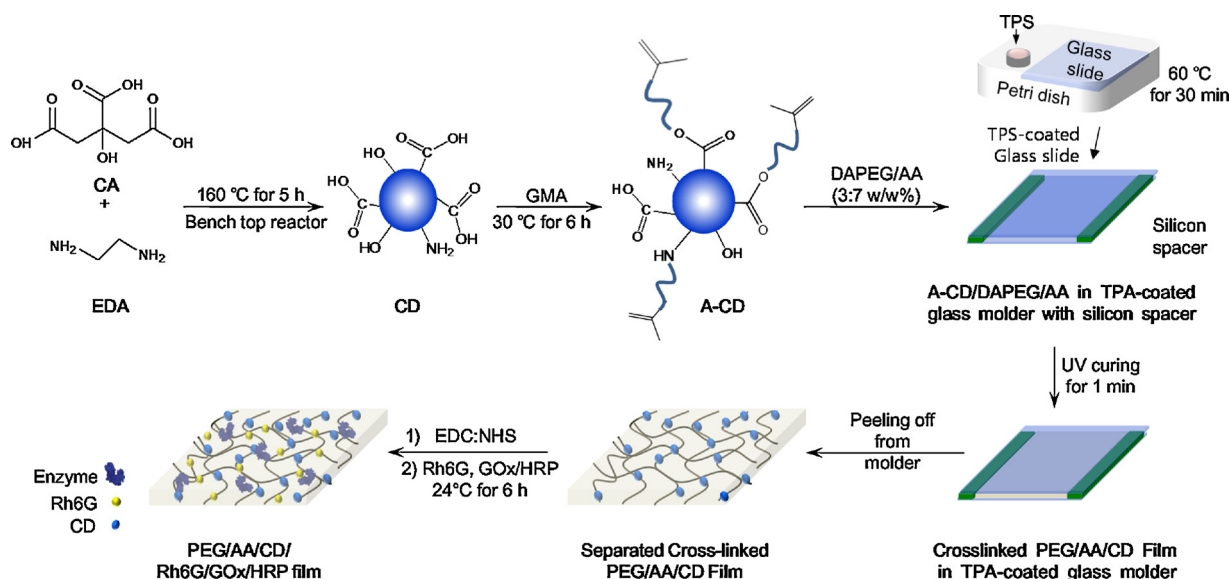
2.4. Preparation of the glucose biosensor film

The DAPEG/AA/CD film was manufactured as shown in Scheme 2. The DAPEG/AA/CD film was fabricated between the glass slides with 200 μ m thick and 0.5 mm wide silicon sheets as spacers; the spacer sheets are placed at the rectangular edges surrounding the sample film, as shown in Scheme 2. The bottom glass slide was fluorine-coated by vapor deposition of TPS (0.2 mL) in a sealed Petri dish (130 \times 130 \times 15 mm³) at 60 °C for 30 min to improve film removal from the glass slide after UV curing, as shown in Scheme 2 [37]. A mixture of A-CD (5.2 $\times 10^{-5}$ wt%), DAPEG (30 wt%), AA (70 wt%), and 2-hydroxy-2-methylpropiophenone (0.01 mL) as a photo cross-linking initiator was poured onto the bottom glass slide and then covered by the top glass slide. The mixture between the glass slides was cured by UV irradiation for 60 s at a distance of 12 cm from the sample. After curing, the crosslinked DAPEG/AA/A-CD film (without the glass slide) was placed in DI water for 1 h to remove unreacted monomers.

2.5. Glucose and human blood serum tests

For glucose detection, an aqueous indicator solution consisting of CDs (0.174 mg/mL), Rh6G (0.04 mg/mL), GOx (27 μ M), and HRP (18 μ M) was prepared. Then, glucose solutions with different concentrations were added to the indicator solution. To investigate the selectivity of glucose detection, various aqueous solutions of biocompounds (lactose, ascorbic acid, urea, Ca²⁺, and Na⁺) were added to the indicator solution at the same final concentrations of 50 μ M. The selectivity of the DAPEG/AA/A-CD/Rh6G/GOx/HRP biosensor solid film was determined according to the method described for the aqueous indicator solution, except that the concentration of all the biological solutions was 100 μ M. All experiments were repeated in triplicate at 24 °C.

For real human blood tests, blood plasma (Sigma-Aldrich) was centrifuged at 5000 rpm for 10 min to remove large molecules and then dissolved in DI water ($\times 40$ dilution). Glucose detection in the centrifuged human blood plasma was tested using the CD/Rh6G/GOx/HRP solution and the DAPEG/AA/A-CD/Rh6G/GOx/HRP film. In addition, the glucose level in human serum was determined by high-performance liquid chromatography (HPLC) [38].



Scheme 2. Schematic for preparation of CDs, A-CDs, and the DAPEG/AA/CD/Rh6G/GOx/HRP Film.

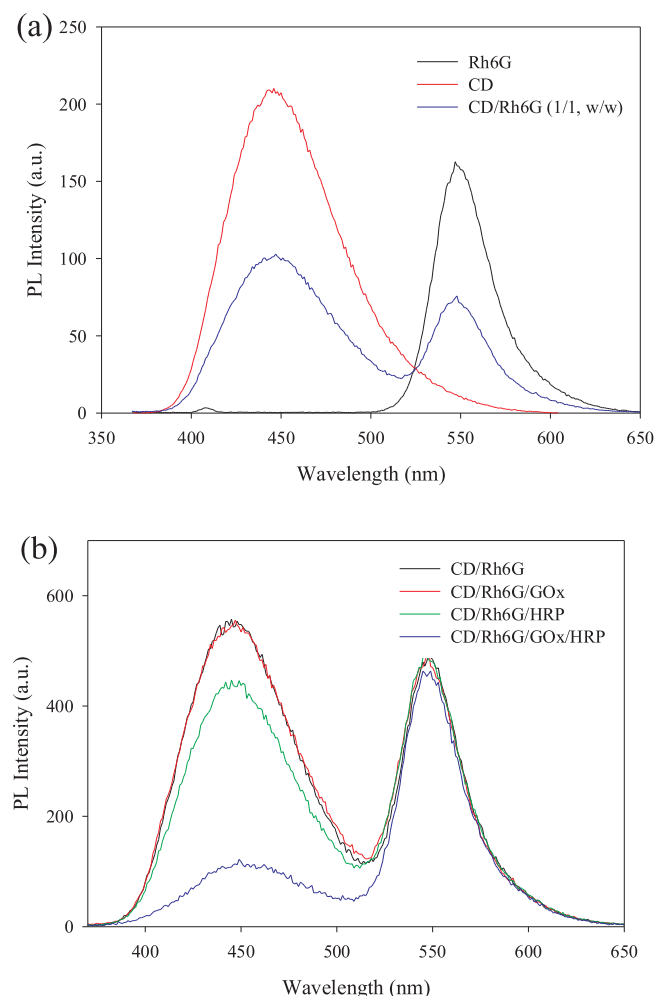


Fig. 1. PL spectra of (a) aqueous solutions (0.002 mg/mL) of CD, Rh6G, and CD/Rh6G (1:1, w/w) ($\lambda_{\text{exc}} = 360$ nm), and (b) aqueous solutions (0.1 mL) of CD/Rh6G (0.174/0.09 mg/mL), CD/Rh6G/GOx (0.174/0.09 (mg/mL)/27 (μM)), CD/Rh6G/HRP (0.174/0.09 (mg/mL)/9 (μM)), and CD/Rh6G/GOx/HRP (0.174/0.09 (mg/mL)/27/9 (μM)) after addition of a glucose solution (1 mM, 2.9 mL).

3. Results and discussion

3.1. Preparation of the CD/GOx/Rh6G aqueous solution as a glucose biosensor

The fluorescence properties of CD, Rh6G, and CD/Rh6G were studied to clarify whether the prepared CDs and Rh6G can exhibit a ratiometric fluorescence color change. Fig. S2a shows the PL spectra of aqueous solutions (0.009 mg/mL) of CDs at different excitation wavelengths (λ_{exc} s). The PL spectra exhibit a maximum at ~ 440 nm. The maximum intensity was observed at $\lambda_{\text{exc}} = 360$ nm, which is consistent with the π - π^* transition of the CDs in the UV-vis spectrum [39]. The PL spectra of aqueous solutions (0.001 mg/mL) of Rh6G at different λ_{exc} s (Fig. S2b) exhibit a maximum at ~ 550 nm. The intensity continuously increases as the λ_{exc} increases. The fluorescence peaks of the CDs and Rh6G at 440 and 550 nm, respectively, are well separated, regardless of λ_{exc} . Thus, further experiments were conducted using $\lambda_{\text{exc}} = 360$ nm, where the CDs show maximum intensity. Fig. 1a shows the PL spectra of aqueous solutions (0.002 mg/mL) of CD, Rh6G, and CD/Rh6G (1:1, w/w) when excited at 360 nm. The PL spectra of the CDs and Rh6G exhibit maximum intensities at 440 and 550 nm, respectively, whereas that of the mixture shows well-separated peaks at 440 and 550 nm. The colors corresponding to 440 and 550 nm are blue and green, respectively,

indicating that the ratiometric color can be tuned by varying the relative intensity of these peaks. The GOx and HRP do not show any fluorescence when excited at 360 nm, as shown in Fig. S3. The PL spectra of CD/Rh6G, CD/Rh6G/GOx, CD/Rh6G/HRP, and CD/Rh6G/GOx/HRP aqueous solutions after the addition of glucose are shown in Fig. 1b; detailed information on the concentrations of these solutions is given in the figure caption. For each tested solution, the PL peak at 550 nm is not affected by glucose addition, indicating that the fluorescence emission of Rh6G is not affected by the enzymatic reactions with glucose. However, the peak at 450 nm corresponding to the CDs is strongly affected by the enzymatic reactions. The mixture of GOx/HRP with glucose quenches the intensity of the CDs significantly, indicating that the produced OH radicals are the main quenchers [40,41]. GOx alone does not quench the PL intensity of the CDs, whereas HRP quenches the PL intensity of the CDs to a small extent. Thus, ratiometric color control is possible with the bienzyme system of GOx/HRP in the CD/Rh6G aqueous solution.

Optimization of the aqueous CD/Rh6G/GOx/HRP solution for glucose biosensor applications was performed. To find the optimum mixing ratio between GOx and HRP, the quenching performance was tested at different mixing ratios. Fig. 2a displays a plot of degree of quenching ($Q_f = (F_0 - F)/F_0$, where F_0 and F are the PL intensities at 450 nm before and after addition of the aqueous glucose solution, respectively) for the CD/GOx/HRP aqueous solution as a function of the mole ratio between GOx and HRP at a constant concentration (34 μM) of GOx + HRP. The Q_f value increases until the mole ratio of GOx/HRP reaches 2.5 and is then saturated, which is consistent with a previously reported result [42]. Thus, for subsequent experiments, we prepared the CD aqueous solution with a 3:1 mole ratio of GOx/HRP. We also tried to determine the time required for fluorescence quenching with GOx/HRP in the aqueous CD solution by examining the intensity at 450 nm of a CD (0.174 mg/mL)/GOx (27 μM)/HRP (9 μM) aqueous solution (0.1 mL) as a function of time after the addition of a glucose solution (10 μM , 2.9 mL) (Fig. 2b). The corresponding normalized PL spectra are shown in Fig. S4. As quenching was almost complete within 10 min, subsequent fluorescence measurements were performed 15 min after glucose addition. To determine the optimum CD concentration (C_{CD}) in water, the Q_f values were determined at different C_{CD} s at a fixed GOx/HRP concentration. The PL spectra of the CD/GOx/HRP aqueous solutions at different C_{CD} s (Fig. S5) and the plot of Q_f as a function of C_{CD} after addition of a glucose solution (Fig. 2c) reveal that Q_f increases as C_{CD} increases, indicating that a low C_{CD} improves quenching. However, as lower resolution data is obtained at low C_{CD} , a C_{CD} of 0.174 mg/mL was chosen for further studies to obtain sufficient fluorescence intensity and a high Q_f (78%).

To determine the optimal distinct fluorescence color change with the aqueous CD/Rh6G solution, the difference in fluorescence color was studied by determining the fluorescence intensity ratio at 550 and 450 nm (I_{550}/I_{450}) for different amounts of Rh6G. Fig. 3a depicts the PL spectra of the CD/Rh6G/GOx/HRP aqueous solution with different concentrations of Rh6G (C_{Rh6G} s) before and after a glucose aqueous solution was added. Before glucose addition, the PL intensity at 550 nm increases as C_{Rh6G} increases with a constant CD intensity at 450 nm. After glucose addition, the PL intensity at 450 nm is significantly quenched, but the PL intensity at 550 nm does not change. The ratio between the PL intensities at 550 and 450 nm (I_{550}/I_{450}) represents the fluorescence color of the solution. The fluorescence color changes from blue to green as the ratio increases. This ratio linearly increases as C_{Rh6G} increases both before and after glucose addition, as shown in Fig. 3b. However, the curve is shifted upward after glucose addition due to the decrease in I_{450} caused by fluorescence quenching of the CDs. A more profound fluorescence change from blue to green is observed when C_{Rh6G} is higher than 0.04 mg/mL (Fig. 3b), and further experiments were performed at this CD/Rh6G (0.174/0.04 mg/mL) concentration. Thus, the optimized indicator solution consisted of CD (0.174 mg/mL)/Rh6G (0.12 mg)/GOx (27 μM)/HRP (9 μM). The concentrations of the

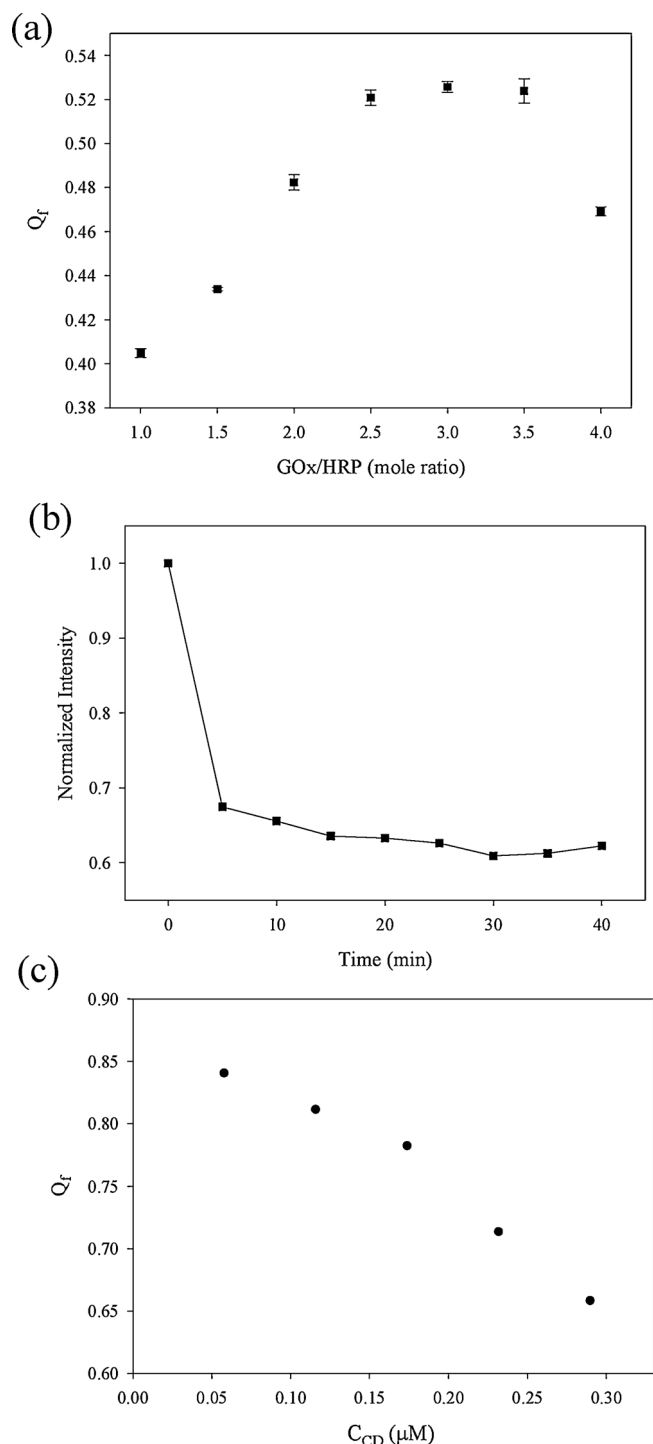


Fig. 2. (a) Q_f of CD aqueous solutions (0.1 mL, 0.57 mg/mL) as a function of the mole ratio between GOx and HRP at a constant concentration (34 μM) of GOx + HRP after addition of an aqueous glucose solution (1 mM, 2.9 mL), (b) normalized intensity of a CD (0.57 mg/mL)/GOx (27 μM)/HRP (9 μM) aqueous solution (0.1 mL) as a function of time after addition of a glucose solution (10 μM , 2.9 mL), and (c) Q_f of CD/GOx (27 μM)/HRP (9 μM) aqueous solutions (0.1 mL) as a function of C_{CD} after addition of a glucose solution (1 mM, 2.9 mL).

CD, Rh6G, GOx, and HRP were not changed unless otherwise mentioned and the CD/Rh6G/GOx/HRP without concentrations in parenthesis indicates the CD(0.174 mg/mL)/Rh6G(0.04 mg/mL)/GOx (27 μM)/HRP (9 μM) aqueous solution in further discussion.

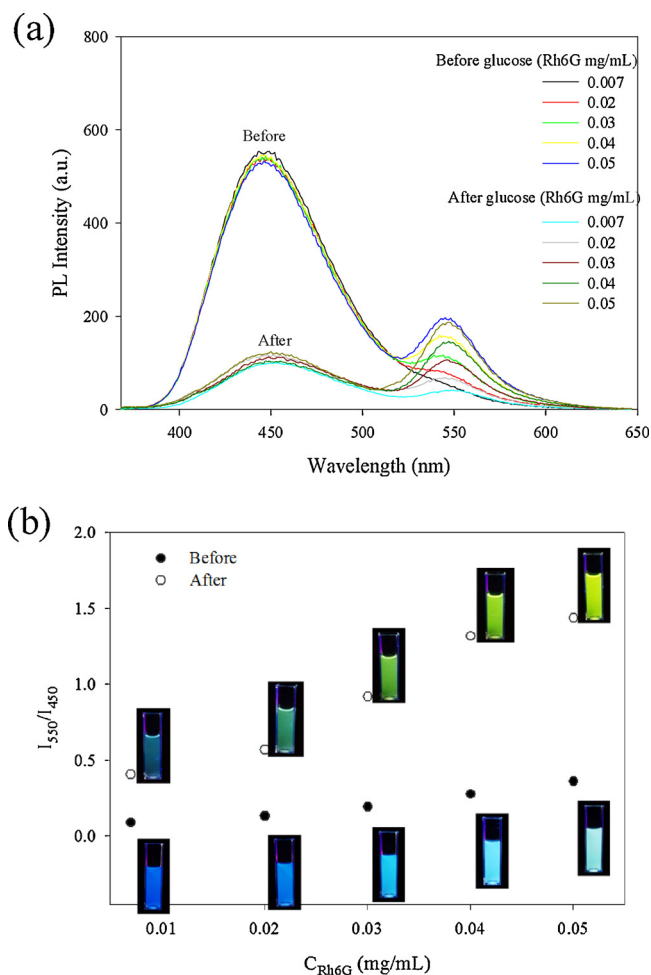


Fig. 3. (a) PL spectra and (b) ratios between PL intensities at 550 and 450 nm (I_{550}/I_{450}) of CD (0.058 mg/mL)/Rh6G/GOx (27 μM)/HRP (9 μM) aqueous solutions (0.1 mL) at C_{Rh6G} of 0.007, 0.02, 0.03, 0.04, and 0.05 mg/mL before and after addition of a glucose aqueous solution (1 mM, 2.9 mL); the insets in (b) show corresponding photographic fluorescence images.

3.2. Glucose biosensor performance of the CD/GOx/Rh6G aqueous solution

Sensitivity was studied with CD/Rh6G/GOx/HRP aqueous solutions which were compared with CD/GOx/HRP aqueous solutions. Fig. 4a and b show the PL spectra of the CD/GOx/HRP (without Rh6G) and CD/Rh6G/GOx/HRP aqueous solutions after a glucose aqueous solution were added with different glucose concentrations (C_g , 0.5–500 μM) and their fluorescence images of the vials, respectively. In the case of the CD/GOx/HRP aqueous solution, the intensity of the peak at 450 nm continuously decreases due to fluorescence quenching so that the intensity of the monochromatic blue fluorescence color decreases. In the case of the CD/Rh6G/GOx/HRP aqueous solution, the peak at 450 nm decreases and the peak at 550 nm does not change as the C_g increases because only CD quenches as mentioned before. Thus, the fluorescence color is continuously changed from blue to green as the C_g increases (Fig. 4b), indicating that the presence of the glucose can be determined by color change instead of the turn-off mode (decreased intensity of the same color). The fluorescence intensity was analyzed for calculating limit of detection (LOD) and linear range. LOD was calculated from three times ($3 \times$) the standard deviation divided by the regression slope, where the standard deviation and the slope are derived from Fig. 4c [43].

Fig. 4c shows the plot of the Q_f (in log scale of C_g) of the CD/GOx/HRP and CD/Rh6G/GOx/HRP aqueous solutions as a function of C_g . The quenching of the solution linearly increases until C_g reaches 500

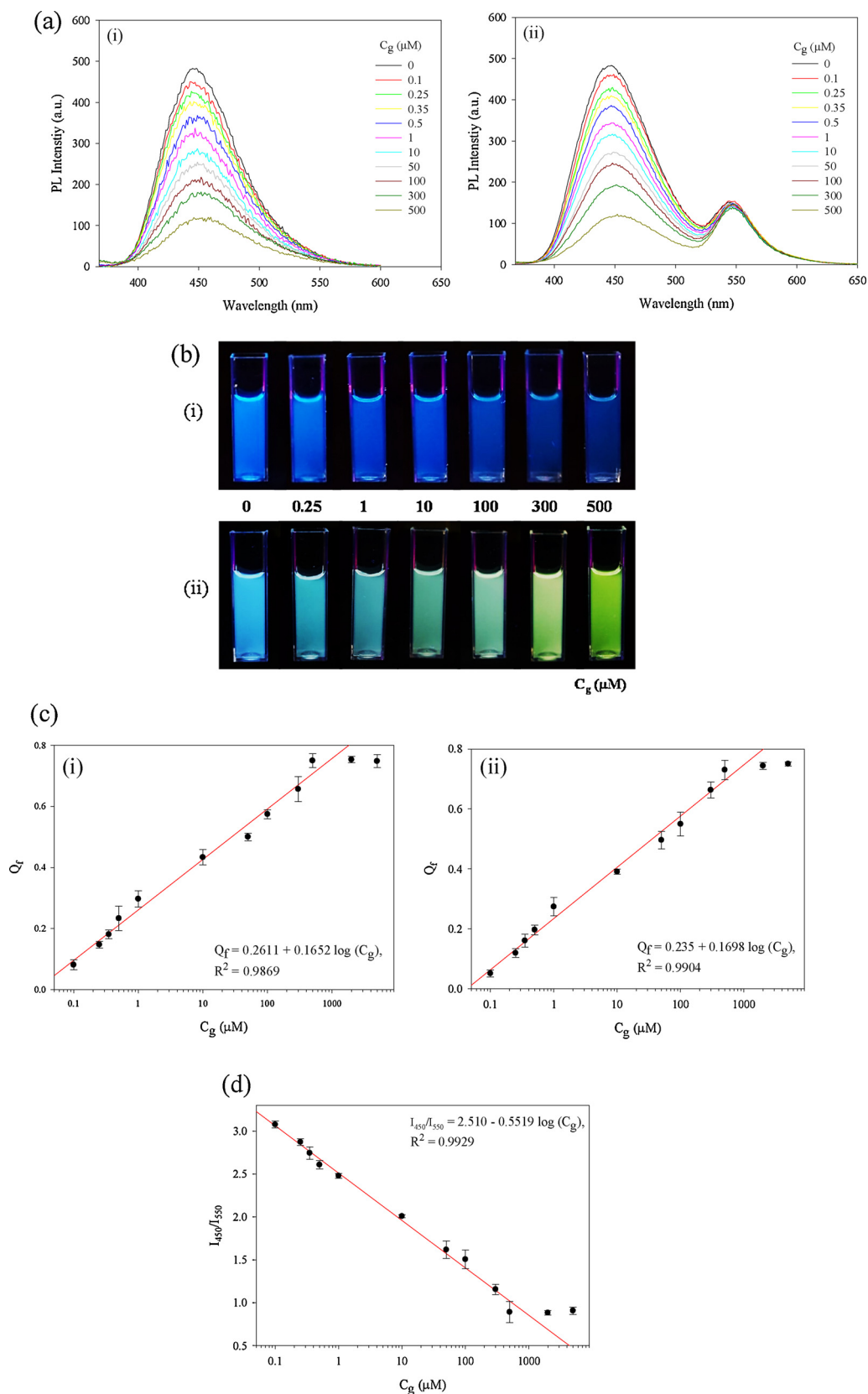


Fig. 4. (a) PL spectra, (b) their fluorescence images, (c) Q_f (in log scale of C_g) of a(i) as a function of C_g for (i) CD/GOx/HRP and (ii) the CD/Rh6G/GOx/HRP aqueous solutions (0.1 mL) in the vials after glucose aqueous solutions (2.9 mL) were added with different C_g s, and (d) I_{450}/I_{550} of the CD/Rh6G/GOx/HRP aqueous solutions as a function of C_g ; numbers in (a, b) represent C_g in μM . Error bars were calculated from measurements from three samples.

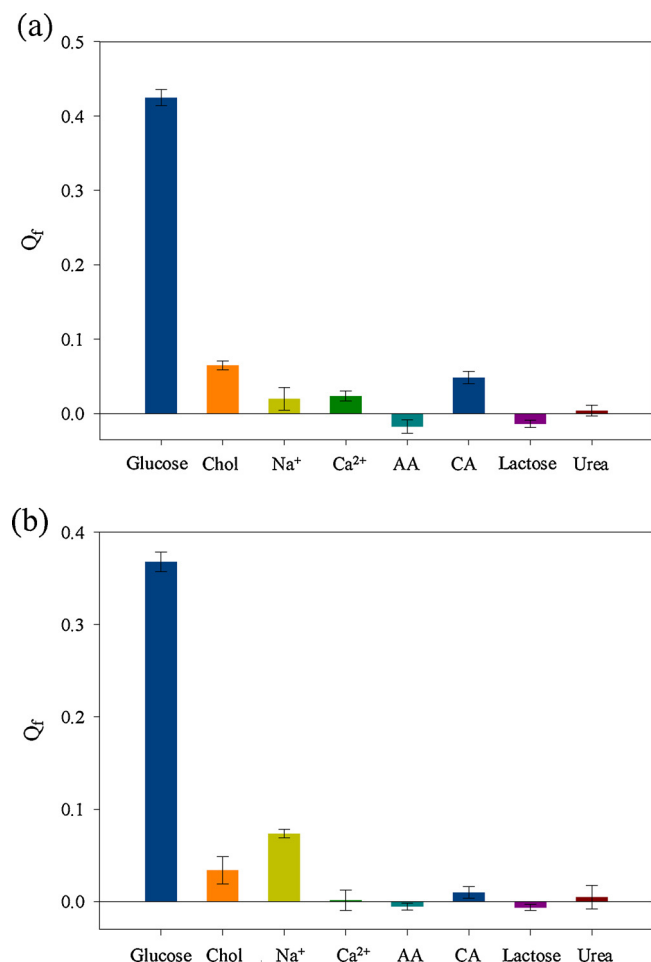


Fig. 5. Q_f of the (a) CD/Rh6G/GOx/HRP aqueous solution (0.1 mL) and (b) DAPEG/AA/A-CD/Rh6G/GOx/HRP film upon addition of glucose, cholesterol, Na^+ and Ca^{2+} ions, ascorbic acid, lactose, and urea aqueous solutions (50 μM for (a) and 100 μM for (b), 2.9 mL). Error bars were calculated from measurements from three samples.

μM so that the linear range is 0.1–500 μM with LOD of 0.04 μM and 0.1–500 μM with LOD of 0.06 μM for CD/GOx/HRP and CD/Rh6G/GOx/HRP aqueous solutions, respectively. Meng et al. reported the glucose biosensor with CDs which were quenched by H_2O_2 in the presence of Fe^{2+} and reported the linear range of 0.05–500 μM with LOD of 0.05 μM , which are similar to our data [26]. One of the merits in using the CD/Rh6G/GOx/HRP aqueous solution as a glucose biosensor is that the inert peak at 550 nm can be used as a reference peak; thus, an initial measurement before adding glucose solution is unnecessary as I_{450}/I_{550} can be used instead of Q_f . As shown in Fig. 4d, I_{450}/I_{550} of the CD/GOx/HRP aqueous solutions has a linear relationship with C_g and thus can be used for determining the glucose concentration without measuring the fluorescence of the CD/Rh6G/GOx/HRP aqueous solution before glucose addition.

The selectivity of the CD/Rh6G/GOx/HRP aqueous solution was tested using the major ingredients of blood. Fig. 5a shows the Q_f values of CD/Rh6G/GOx/HRP aqueous solutions when glucose, cholesterol, Na^+ and Ca^{2+} ions, ascorbic acid, lactose, and urea aqueous solutions were added. Little fluorescence quenching occurs except upon addition of glucose; AA and lactose even slightly increase the fluorescence intensity. This result indicated that the CD/Rh6G/GOx/HRP aqueous solution is quite selective for glucose.

3.3. Preparation of the glucose biosensor solid film

A PAA film crosslinked with DAPEG was prepared as a matrix film for the glucose biosensor. PAA films with less than 10 wt% DAPEG were sticky owing to a low degree of crosslinking. In contrast, PAA films with more than 20 wt% DAPEG showed good film formation and good immobilization of CDs, GOx, and HRP. However, the film with 20 wt% DAPEG was somewhat sticky and wrinkled when the aqueous glucose solution was dropped onto it. Thus, the PAA film crosslinked with 30 wt % DAPEG was used for fabricating the glucose sensor film. To incorporate CDs into the PAA film, the A-CDs were used during UV polymerization. The A-CDs were synthesized as shown in Scheme 2, and Fig. 6a depicts the FT-IR spectra of the CDs and A-CDs. The peaks in the FT-IR spectrum of the CDs at 2919, 1687, 1584, and 1195 cm^{-1} correspond to C–H stretching, C=O stretching, N–H bending, and C–O stretching, respectively, consistent with reported data [36]. The FT-IR spectrum of the A-CDs shows additional peaks at 1628 and 1293 cm^{-1} , which are due to C=C stretching and C–O stretching (esters), respectively, indicating that reactive acrylic groups were introduced by the GMA reaction. A mixture of the A-CDs (5.2×10^{-5} wt%) and AA/DAPEG (7:3, w/w) was UV cured between sandwiched glass slides with a gap of 0.2 mm, producing a uniform film with good stability, as shown in Fig. 6b. For functionalization with GOx and HRP, the aqueous EDC:NHS solution was placed on the crosslinked film to activate the film and then GOx and HRP were immobilized in the film. To verify whether GOx and HRP were covalently immobilized in the film, water into which the film was inserted was tested. Fig. S6 displays the UV spectra of water, GOx/HRP (3:1 mole ratio, 3 wt%), and water after immersion of the DAPEG/AA/A-CD/GOx/HRP film in 20 mL water for 6 h. The UV spectrum of the HRP/GOx mixture shows peaks at 390 and 480 nm, whereas that of the water in which the prepared film was immersed does not show any peaks, indicating that the enzymes are firmly immobilized in the film. Photographic images of the flexible DAPEG/AA/A-CD/GOx/HRP film in the absence and presence of UV light at 365 nm (Fig. 6b) reveal clear and uniform fluorescence emission, indicating that the CDs were successfully immobilized in the film. Thus, the optimized biosensor film consisted of DAPEG/AA (3:7, w/w)/A-CD (5.2×10^{-5} wt%)/Rh6G (1.6×10^{-4})/GOx/HRP (3:1 mole ratio, 0.16 wt%). The composition of DAPEG and AA and the concentrations of CD, Rh6G, GOx, and HRP were not changed unless otherwise mentioned, and hereafter, the use of DAPEG/AA/A-CD/Rh6G/GOx/HRP without concentrations in parentheses indicates this film.

3.4. Performance of the glucose biosensor solid film

Sensitivity and the ratiometric fluorescence color change were studied with the optimized DAPEG/AA/A-CD/GOx/HRP film. Fig. 7a and b show the PL spectra of the film after the addition of glucose aqueous solutions with different C_g s and the corresponding fluorescence images, respectively. The fluorescence color continuously changes from blue to green as C_g increases (Fig. 7b), indicating that the presence of glucose can be determined by the color change, similar to behavior of the CD/Rh6G/GOx/HRP aqueous solution. The fluorescence intensity was analyzed to calculate the LOD and the linear range. As shown in the plot of Q_f of the film as a function of C_g (log scale) (Fig. 7c(i)), the quenching linearly increases until C_g reaches 500 μM , corresponding to a linear range of 0.5–500 μM with an LOD of 0.08 μM . As a similar linear relationship was obtained for I_{450}/I_{550} of the DAPEG/AA/GMA-CD/GOx/HRP film as a function of C_g (Fig. 7c(ii)), this ratio can be used to determine the glucose concentration without measuring the fluorescence before glucose addition. Fig. 5b shows the Q_f of the DAPEG/AA/A-CD/GOx/HRP film upon addition of glucose, cholesterol, Na^+ and Ca^{2+} ions, ascorbic acid, lactose, and urea aqueous solutions. Similar to the data for the aqueous solution, little fluorescence quenching occurs, except in the presence of glucose. This result indicated that the DAPEG/AA/A-CD/GOx/HRP film is also quite selective for glucose. The

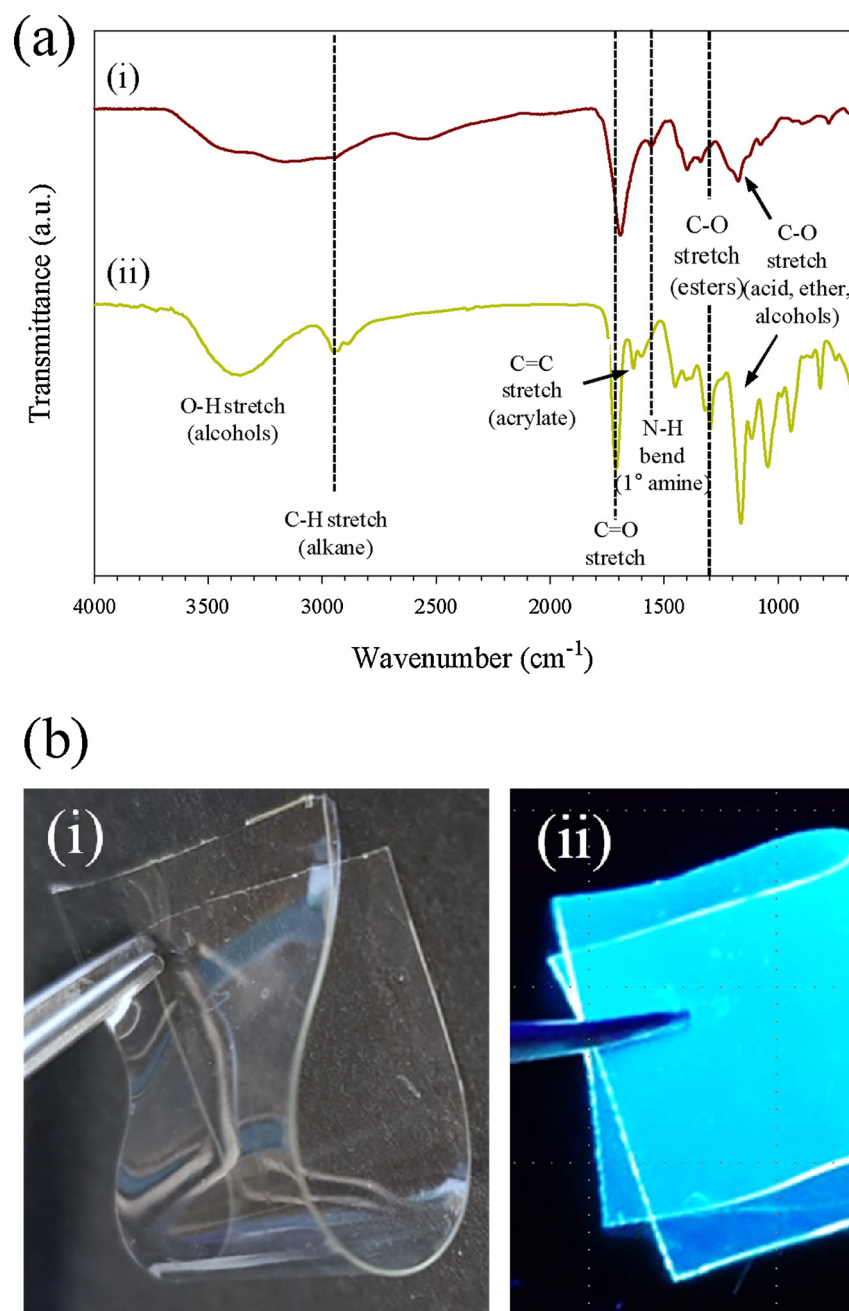


Fig. 6. (a) FT-IR spectra of (i) CDs and (ii) A-CDs, and (b) photographic images of the flexible DAPEG/AA/A-CD/Rh6G/GOx/HRP film in the (i) absence and (ii) presence of UV light at 365 nm.

reusability of the DAPEG/AA/A-CD/Rh6G/GOx/HRP film was tested after treating it with the glucose solution. Fig. S7 shows the fluorescence image after adding glucose aqueous solutions (2.9 mL) at $C_g = 500 \mu\text{M}$ and washing with water two times. We determined that the fluorescence of the film was not recovered, indicating that once the CD was quenched with the radicals produced from the enzymatic reaction, the fluorescence of CD was not recovered. Selectivity was tested by a mixture of cholesterol, Na^+ and Ca^{2+} ions, ascorbic acid, lactose, and urea aqueous solutions. Fig. 8 shows the Q_f values of the CD/Rh6G/GOx/HRP aqueous solutions and the DAPEG/AA/A-CD/Rh6G/GOx/HRP film when the mixture of cholesterol, Na^+ and Ca^{2+} ions, ascorbic acid, lactose, and urea aqueous solutions was added with and without glucose. Little fluorescence quenching occurs without glucose whereas significant fluorescence quenching was observed with glucose. This result indicates that the CD/Rh6G/GOx/HRP aqueous solution and the

DAPEG/AA/A-CD/Rh6G/GOx/HRP film are considerably selective to glucose.

Finally, we tested the ability of the CD/Rh6G/GOx/HRP aqueous solution and the DAPEG/AA/A-CD/Rh6G/GOx/HRP film to detect glucose in diluted human plasma serum ($\times 40$ with DI water). The original amount of glucose in the undiluted sample was 5.32 mM, as measured by HPLC [32]. Thus, known amounts of glucose were added to the serum samples after centrifugation to remove large molecules. The glucose content in the spiked serum samples was determined from the fluorescence spectra of the CD/Rh6G/GOx/HRP aqueous solution (Fig. S8a) and the DAPEG/AA/A-CD/Rh6G/GOx/HRP film (Fig. S8b) using calibration curves (Fig. 4c(ii) and Fig. 7c(i)). Table S1 shows the LOD and linear ranges of the reported sensors. The developed sensor has a good LOD; however, its linear range is slightly narrow as compared to other sensors [44–47]. Table 1 shows the added and measured

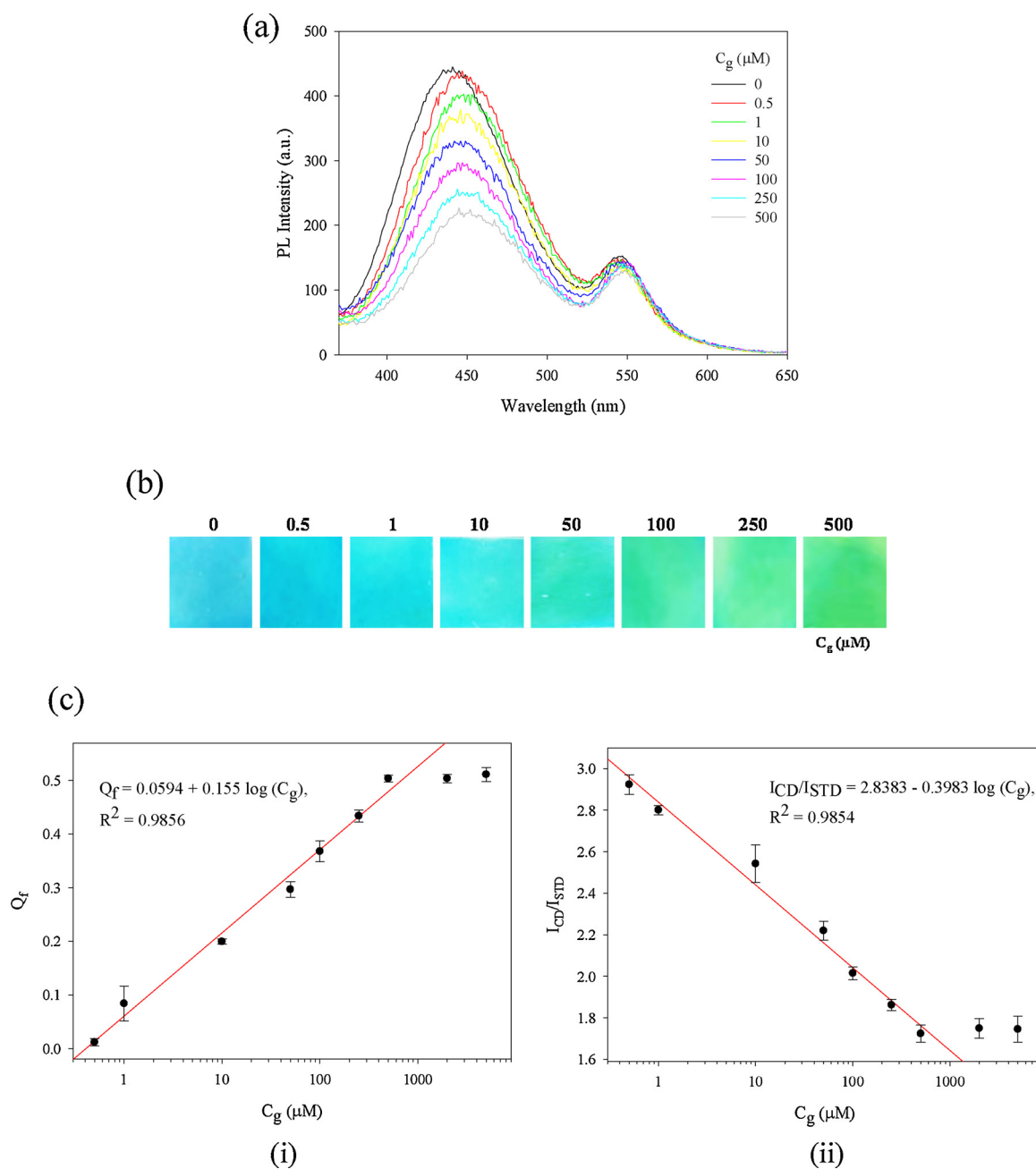


Fig. 7. (a) PL spectra, (b) corresponding fluorescence images, and (c) (i) Q_f and (ii) I_{450}/I_{550} as a function of C_g (log scale) for the DAPEG/AA/A-CD/Rh6G/GOx/HRP film after addition of glucose aqueous solutions (2.9 mL) with different C_g s; the numbers in (a, b) represent C_g in μM . Error bars were calculated from measurements from three samples.

amounts of glucose in human serum. Recovery ratios (determined as (measured amount - original amount)/added amount) of 109.36% and 104.73% were obtained for serum samples at C_g (added glucose) = 40 and 300 μM , respectively, using the CD/Rh6G/GOx/HRP aqueous solution. Using the DAPEG/AA/A-CD/Rh6G/GOx/HRP film, recovery ratios of 120.83% and 107.26% were obtained for the samples at C_g = 40 and 300 μM , respectively, indicating that this glucose biosensor can be used with real human blood samples. Although deviations from 100% were observed, possibly reflecting interference from other biomaterials in human serum, these deviations were relatively small.

4. Conclusion

A ratiometric fluorescence method was successfully developed for glucose detection with CD and Rh6G fluorophores through a bienzyme

(GOx and HRP) system in the form of an aqueous solution or a solid-state PAA film crosslinked with DAPEG. The blue-emitting CDs showed fluorescence quenching, whereas green-emitting Rh6G was inert to the bienzymatic reaction of GOx and HRP with glucose, resulting in a continuous fluorescence color change from blue to green as the glucose concentration increased in both the aqueous and solid-state systems. Both the optimized aqueous solution and film showed good glucose detection performance in terms of sensitivity, selectivity, and stability. In particular, the solid-state film can be carried in the dry state and used whenever needed to test blood samples. Thus, these ratiometric fluorescence systems allow the realization of convenient and practical biosensor applications using biocompatible and nontoxic CDs.

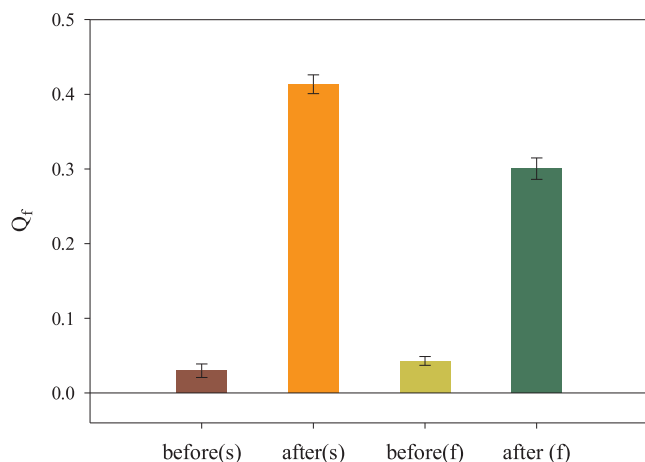


Fig. 8. Q_f values of CD/Rh6G/GOx/HRP aqueous solutions and DAPEG/AA/A-CD/Rh6G/GOx/HRP films when a mixture of cholesterol, Na^+ and Ca^{2+} ions, ascorbic acid, lactose, and urea aqueous solutions was added with and without glucose; the concentration of all analytes was 50 μM ; “before” and “after” indicate the aqueous solution without and with glucose, respectively, and “s” and “f” denote the aqueous solution and the film samples, respectively.

Table 1

Amounts of Glucose in Human Blood Plasma Measured with the CD/Rh6G/GOx/HRP Aqueous Solution and the DAPEG/AA/A-CD/Rh6G/GOx/HRP Film.

Samples	glucose (μM)			Recovery ^b (%)	RSD ^c (n = 3, %)
	Original ^a	Added	Measured		
1. (solution)	133	40	176.7	102.1	4.10
2. (solution)	133	300	447.2	103.3	2.71
3. (film)	133	40	181.3	104.8	7.88
4. (film)	133	300	454.8	105.0	4.16

^a Original amount of glucose in human blood serum.

^b Recovery = (Measured glucose)/(Original glucose + Add glucose) \times 100%.

^c RSD = relative standard deviation.

Notes

The authors declare no competing financial interest.

Acknowledgment

This work was supported by the National Research Foundation of Korea (2017R1A2B2006818).

Appendix A. Supplementary data

Supplementary material related to this article can be found, in the online version, at doi:<https://doi.org/10.1016/j.snb.2018.11.055>.

References

- [1] S. Wild, G. Roglic, A. Green, R. Sicree, H. King, Global prevalence of diabetes: estimates for the year 2000 and projections for 2030, *Diabetes Care* 27 (2004) 1047–1053.
- [2] L.C. Clark Jr, C. Lyons, Electrode systems for continuous monitoring in cardiovascular surgery, *Ann. N. Y. Acad. Sci.* 102 (1962) 29–45.
- [3] S.J. Updike, G.P. Hicks, The enzyme electrode, *Nature* 214 (1967) 986–988.
- [4] A. Hiratsuka, K. Fujisawa, H. Murguruma, Amperometric biosensor based on glucose dehydrogenase and plasma-polymerized thin films, *Anal. Sci.* 24 (2008) 483–486.
- [5] J.P. Chambers, B.P. Arulanandam, L.L. Matta, A. Weis, J.J. Valdes, Biosensor recognition elements, *Curr. Issues Mol. Biol.* 10 (2008) 1–12.
- [6] S.S. Iqbal, M.W. Mayo, J.G. Bruno, B.V. Bronk, C.A. Batt, J.P. Chambers, A review of molecular recognition technologies for detection of biological threat agents, *Biosens. Bioelectron.* 15 (2000) 549–578.
- [7] J.D. Newman, A.P. Turner, *Biosensors: principles and practice*, Essays Biochem. 27 (1992) 147–159.
- [8] K. Habermuller, M. Mosbach, W. Schuhmann, Electron-transfer mechanisms in amperometric biosensors, *Fresenius J. Anal. Chem.* 366 (2000) 560–568.
- [9] J.E. Pearson, A. Gill, P. Vadgama, Analytical aspects of biosensors, *Ann. Clin. Biochem.* 37 (Pt 2) (2000) 119–145.
- [10] D.R. Thevenot, K. Toth, R.A. Durst, G.S. Wilson, Electrochemical biosensors: recommended definitions and classification, *Biosens. Bioelectron.* 16 (2001) 121–131.
- [11] J. Qian, C. Ren, Wang C, W. Chen, X. Lu, H. Li, K. Wang, Magnetically controlled fluorescence aptasensor for simultaneous determination of ochratoxin A and aflatoxin B1, *Anal. Chim. Acta* 1019 (2018) 119–127.
- [12] L. Long, M. Huang, N. Wang, Y. Wu, K. Wang, A. Gong, J.L. Sessler, A mitochondria-specific fluorescent probe for visualizing endogenous hydrogen cyanide fluctuations in neurons, *J. Am. Chem. Soc.* 140 (5) (2018) 1870–1875.
- [13] Y. Li, L. Sun, J. Qian, L. Long, H. Li, Q. Liu, K. Wang, Fluorescent “on-off-on” switching sensor based on CdTe quantum dots coupled with multiwalled carbon nanotubes@ graphene oxide nanoribbons for simultaneous monitoring of dual foreign DNAs in transgenic soybean, *Biosens. Bioelectron.* 92 (2017) 26–32.
- [14] J. Qian, K. Wang, C. Ren, C. Ren, Q. Liu, N. Hao, K. Wang, Ratiometric fluorescence nanosensor for selective and visual detection of cadmium ions using quencher displacement-induced fluorescence recovery of CdTe quantum dots-based hybrid probe, *Sens. Actuators B Chem.* 241 (2017) 1153–1160.
- [15] J. Qian, M. Hua, C. Wang, K. Wang, Q. Liu, N. Hao, K. Wang, Fabrication of l-cysteine-capped CdTe quantum dots based ratiometric fluorescence nanosensor for onsite visual determination of trace TNT explosive, *Anal. Chim. Acta* 946 (2016) 80–87.
- [16] K. Wang, J. Qian, D. Jiang, Z. Yang, Du X, K. Wang, Onsite naked eye determination of cysteine and homocysteine using quencher displacement-induced fluorescence recovery of the dual-emission hybrid probes with desired intensity ratio, *Biosens. Bioelectron.* 65 (2015) 83–90.
- [17] A. Heller, Amperometric biosensors, *Curr. Opin. Biotechnol.* 7 (1996) 50–54.
- [18] A.P. Turner, B. Chen, S.A. Piletsky, In vitro diagnostics in diabetes: meeting the challenge, *Clin. Chem.* 45 (1999) 1596–1601.
- [19] E. D’costa, I. Higgins, A. Turner, Quinoprotein glucose dehydrogenase and its application in an amperometric glucose sensor, *Biosensors* 2 (1986) 71–87.
- [20] C.P. Price, Point-of-care testing in diabetes mellitus, *Clin. Chem. Lab. Med.* 41 (2003) 1213–1219.
- [21] A. Heller, B. Feldman, Electrochemical glucose sensors and their applications in diabetes management, *Chem. Rev.* 108 (2008) 2482–2505.
- [22] S.B. Bankar, M.V. Bule, R.S. Singhal, L. Ananthanarayan, Glucose oxidase—an overview, *Biotechnol. Adv.* 27 (2009) 489–501.
- [23] J.A. Tamada, S. Garg, L. Jovanovic, K.R. Pitzer, S. Fermi, R.O. Potts, Noninvasive glucose monitoring: comprehensive clinical results, *Cygnus Res. Team, JAMA* 282 (1999) 1839–1844.
- [24] M.J. McShane, Potential for glucose monitoring with nanoengineered fluorescent biosensors, *Diabetes Technol. Ther.* 4 (2002) 533–538.
- [25] R.M. Clegg, Fluorescence resonance energy transfer, *Curr. Opin. Biotechnol.* 6 (1995) 103–110.
- [26] H. Zhai, T. Feng, L. Dong, L. Wang, X. Wang, H. Liu, et al., Development of dual-emission ratiometric probe-based on fluorescent silica nanoparticle and CdTe quantum dots for determination of glucose in beverages and human body fluids, *Food Chem.* 204 (2016) 444–452.
- [27] S. Qiao, H. Li, H. Li, J. Liu, W. Kong, Q. Hu, et al., Label-free carbon quantum dots as photoluminescence probes for ultrasensitive detection of glucose, *RSC Adv.* 5 (2015) 69042–69046.
- [28] H. Xia, J. Hu, J. Tang, K. Xu, X. Hou, P. Wu, A RGB-type quantum dot-based sensor array for sensitive visual detection of trace formaldehyde in air, *Sci. Rep.* 6 (2016) 36794.
- [29] L. Chen, L. Sun, J. Zheng, J. Dai, Y. Wu, X. Dai, et al., Dual-emission ratiometric fluorescence detection of aspirin in human saliva: onsite naked-eye detection and high stability, *New J. Chem.* 41 (2017) 14551–14556.
- [30] S.N. Baker, G.A. Baker, Luminescent carbon nanodots: emergent nanolights, *Angew. Chem. Int. Ed. Engl.* 49 (2010) 6726–6744.
- [31] J. Wei, L. Qiang, J. Ren, X. Ren, F. Tang, X. Meng, Fluorescence turn-off detection of hydrogen peroxide and glucose directly using carbon nanodots as probes, *Anal. Methods* 6 (2014) 1922–1927.
- [32] J. Zhao, C. Liu, Y. Li, J. Liang, J. Liu, T. Qian, et al., Preparation of carbon quantum dots based high photostability luminescent membranes, *Luminescence* 32 (2017) 625–630.
- [33] B. Chen, J. Feng, White-light-emitting polymer composite film based on carbon dots and lanthanide complexes, *J. Phys. Chem. C* 119 (2015) 7865–7872.
- [34] T. Wu, Y. Li, D.S. Lee, Chitosan-based composite hydrogels for biomedical applications, *Macromol. Res.* 25 (2017) 480–488.
- [35] D. Qu, M. Zheng, L. Zhang, H. Zhao, Z. Xie, X. Jing, et al., Formation mechanism and optimization of highly luminescent N-doped graphene quantum dots, *Sci. Rep.* 4 (2014) 5294.
- [36] M.-J. Cho, S.-Y. Park, Preparation of poly (styrene)-b-poly (acrylic acid)-coupled carbon dots and their applications, *ACS Appl. Mater. Interfaces* 9 (2017) 24169–24178.
- [37] R. Gordon, Chemical vapor deposition of coatings on glass, *J. Non. Cryst. Solids* 218 (1997) 81–91.
- [38] M. Khan, S.-Y. Park, Liquid crystal-based biosensor with backscattering interferometry: a quantitative approach, *Biosens. Bioelectron.* 87 (2017) 976–983.
- [39] X.M. Li, S.L. Zhang, S.A. Kulnich, Y.L. Liu, H.B. Zeng, Engineering surface states of carbon dots to achieve controllable luminescence for solid-luminescent composites

- and sensitive Be^{2+} detection, *Sci. Rep.* 4 (2014) 4976.
- [40] S.X. Chen, P. Schopfer, Hydroxyl-radical production in physiological reactions: a novel function of peroxidase, *Eur. J. Biochem.* 260 (3) (1999) 726–735.
- [41] H.-I. Park, S.-Y. Park, Smart fluorescent hydrogel glucose biosensing microdroplets with dual-mode fluorescence quenching and size reduction, *ACS Appl. Mater. Interfaces* 10 (2018) 30172–30179.
- [42] M. Khan, S.-Y. Park, Glucose biosensor based on GOx/HRP bienzyme at liquid–crystal/aqueous interface, *J. Colloid Interface Sci.* 457 (2015) 281–288.
- [43] A. Shrivastava, V.B. Gupta, Methods for the determination of limit of detection and limit of quantitation of the analytical methods, *Chron. Young Sci.* 2 (1) (2011) 21.
- [44] S.K. Vaishnav, J. Korram, R. Nagwanshi, K.K. Ghosh, M.L. Satnami, Mn^{2+} doped-CdTe/ZnS modified fluorescence nanosensor for detection of glucose, *Sens. Actuators B: Chem.* 245 (2017) 196–204.
- [45] J. Liu, L. Lu, A. Li, J. Tang, S. Wang, S. Xu, L. Wang, Simultaneous detection of hydrogen peroxide and glucose in human serum with upconversion luminescence, *Biosens. Bioelectron.* 68 (2015) 204–209.
- [46] J.-L. Ma, B.-C. Yin, X. Wu, B.-C. Ye, Simple and cost-effective glucose detection based on carbon nanodots supported on silver nanoparticles, *Anal. Chem.* 89 (2016) 1323–1328.
- [47] C. Zhang, Y. Yuan, S. Zhang, Y. Wang, Z. Liu, Biosensing platform based on fluorescence resonance energy transfer from upconverting nanocrystals to graphene oxide, *Angew. Chem. Int. Ed.* 50 (2011) 6851–6854.